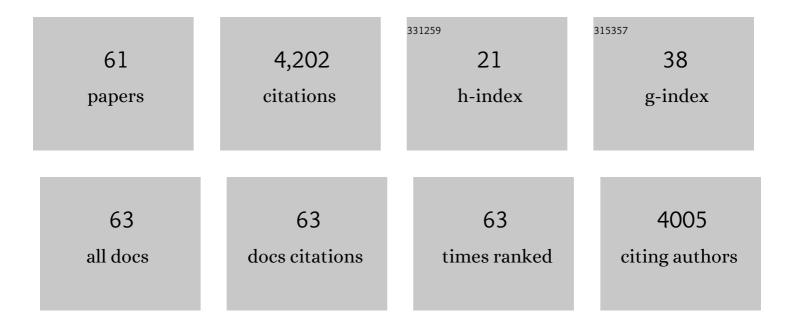
List of Publications by Year in descending order

Source: https://exaly.com/author-pdf/11235782/publications.pdf Version: 2024-02-01



#	Article	IF	CITATIONS
1	Temporal Relationship Between Visual Field, Retinal and Microvascular Pathology Following ¹²⁵ I-Plaque Brachytherapy for Uveal Melanoma. , 2021, 62, 3.		7
2	Utility of Spectral-Domain Optical Coherence Tomography in Differentiating Papilledema From Pseudopapilledema: A Prospective Longitudinal Study. Journal of Neuro-Ophthalmology, 2021, 41, e509-e515.	0.4	5
3	AxonDeep: Automated Optic Nerve Axon Segmentation in Mice With Deep Learning. Translational Vision Science and Technology, 2021, 10, 22.	1.1	11
4	A Deep-Learning Approach for Automated OCT En-Face Retinal Vessel Segmentation in Cases of Optic Disc Swelling Using Multiple En-Face Images as Input. Translational Vision Science and Technology, 2020, 9, 17.	1.1	9
5	The Effect of Acetazolamide and Weight Loss on Intraocular Pressure in Idiopathic Intracranial Hypertension Patients. Journal of Glaucoma, 2019, 28, 352-356.	0.8	4
6	A machine-learning graph-based approach for 3D segmentation of Bruch's membrane opening from glaucomatous SD-OCT volumes. Medical Image Analysis, 2017, 39, 206-217.	7.0	28
7	Incorporation of gradient vector flow field in a multimodal graph-theoretic approach for segmenting the internal limiting membrane from glaucomatous optic nerve head-centered SD-OCT volumes. Computerized Medical Imaging and Graphics, 2017, 55, 87-94.	3.5	16
8	Optical Coherence Tomography Analysis Based Prediction of Humphrey 24-2 Visual Field Thresholds in Patients With Glaucoma. , 2017, 58, 3975.		34
9	Peripapillary Retinal Pigment Epithelium Layer Shape Changes From Acetazolamide Treatment in the Idiopathic Intracranial Hypertension Treatment Trial. , 2017, 58, 2554.		29
10	The Pattern of Visual Fixation Eccentricity and Instability in Optic Neuropathy and Its Spatial Relationship to Retinal Ganglion Cell Layer Thickness. , 2016, 57, OCT429.		13
11	Retinal Ganglion Cell Layer Thinning Within One Month of Presentation for Non-Arteritic Anterior Ischemic Optic Neuropathy. , 2016, 57, 3588.		37
12	Multimodal registration of SD-OCT volumes and fundus photographs using histograms of oriented gradients. Biomedical Optics Express, 2016, 7, 5252.	1.5	21
13	Quantitative measurement of retinal ganglion cell populations via histology-based random forest classification. Experimental Eye Research, 2016, 146, 370-385.	1.2	23
14	RetFM-J, an ImageJ-based module for automated counting andÂquantifying features of nuclei in retinal whole-mounts. Experimental Eye Research, 2016, 146, 386-392.	1.2	24
15	Retinal ganglion cell layer thinning within one month of presentation for optic neuritis. Multiple Sclerosis Journal, 2016, 22, 641-648.	1.4	77
16	Causes and Prognosis of Visual Acuity Loss at the Time of Initial Presentation in Idiopathic Intracranial Hypertension. , 2015, 56, 3850.		70
17	Automated construction of arterial and venous trees in retinal images. Journal of Medical Imaging, 2015, 2, 044001.	0.8	35
18	Movement of Retinal Vessels to Optic Nerve Head with Intraocular Pressure Elevation in a Child. Ophthalmology, 2015, 122, 1532-1534.	2.5	3

#	Article	IF	CITATIONS
19	Multimodal Segmentation of Optic Disc and Cup From SD-OCT and Color Fundus Photographs Using a Machine-Learning Graph-Based Approach. IEEE Transactions on Medical Imaging, 2015, 34, 1854-1866.	5.4	62
20	Relationships of Retinal Structure and Humphrey 24-2 Visual Field Thresholds in Patients With Glaucoma. Investigative Ophthalmology and Visual Science, 2015, 56, 259-271.	3.3	43
21	Automated Method for Identification and Artery-Venous Classification of Vessel Trees in Retinal Vessel Networks. PLoS ONE, 2014, 9, e88061.	1.1	66
22	Automated 3D Segmentation of Intraretinal Surfaces in SD-OCT Volumes in Normal and Diabetic Mice. Translational Vision Science and Technology, 2014, 3, 8.	1.1	15
23	Incorporation of learned shape priors into a graph-theoretic approach with application to the 3D segmentation of intraretinal surfaces in SD-OCT volumes of mice. Proceedings of SPIE, 2014, , .	0.8	0
24	Graph Algorithmic Techniques for Biomedical Image Segmentation. , 2014, , 3-45.		0
25	Automated 3D Segmentation of Multiple Surfaces with a Shared Hole: Segmentation of the Neural Canal Opening in SD-OCT Volumes. Lecture Notes in Computer Science, 2014, 17, 739-746.	1.0	16
26	Splat Feature Classification With Application to Retinal Hemorrhage Detection in Fundus Images. IEEE Transactions on Medical Imaging, 2013, 32, 364-375.	5.4	147
27	A combined machine-learning and graph-based framework for the segmentation of retinal surfaces in SD-OCT volumes. Biomedical Optics Express, 2013, 4, 2712.	1.5	46
28	Multimodal segmentation of optic disc and cup from stereo fundus and SD-OCT images. Proceedings of SPIE, 2013, , .	0.8	8
29	Effect of Age on Individual Retinal Layer Thickness in Normal Eyes as Measured With Spectral-Domain Optical Coherence Tomography. , 2013, 54, 4934.		157
30	Reproducibility of SD-OCT–Based Ganglion Cell–Layer Thickness in Glaucoma Using Two Different Segmentation Algorithms. , 2013, 54, 6998.		22
31	Optimal Multiple Surface Segmentation With Shape and Context Priors. IEEE Transactions on Medical Imaging, 2013, 32, 376-386.	5.4	99
32	Extending the XNAT archive tool for image and analysis management in ophthalmology research. Proceedings of SPIE, 2013, , .	0.8	0
33	Automated Detection of Malarial Retinopathy-Associated Retinal Hemorrhages. , 2012, 53, 6582.		21
34	Quantitative Evaluation of Papilledema from Stereoscopic Color Fundus Photographs. , 2012, 53, 4490.		18
35	Automated artery-venous classification of retinal blood vessels based on structural mapping method. Proceedings of SPIE, 2012, , .	0.8	10
36	Early Neurodegeneration in the Retina of Type 2 Diabetic Patients. , 2012, 53, 2715.		273

#	Article	IF	CITATIONS
37	Registration of 3D spectral OCT volumes combining ICP with a graph-based approach. , 2012, , .		10
38	Distribution of Damage to the Entire Retinal Ganglion Cell Pathway. JAMA Ophthalmology, 2012, 130, 1118.	2.6	23
39	Multimodal Retinal Vessel Segmentation From Spectral-Domain Optical Coherence Tomography and Fundus Photography. IEEE Transactions on Medical Imaging, 2012, 31, 1900-1911.	5.4	43
40	A Method for an Image-Analysis-Based Two-Dimensional Computational Fluid Dynamics Simulation of Moving Fish. Transactions of the American Fisheries Society, 2012, 141, 185-198.	0.6	3
41	Incorporation of texture-based features in optimal graph-theoretic approach with application to the 3D segmentation of intraretinal surfaces in SD-OCT volumes. , 2012, , .		7
42	2-D Pattern of Nerve Fiber Bundles in Glaucoma Emerging from Spectral-Domain Optical Coherence Tomography. , 2012, 53, 483.		20
43	Automated Quantification of Volumetric Optic Disc Swelling in Papilledema Using Spectral-Domain Optical Coherence Tomography. , 2012, 53, 4069.		77
44	Automated method for the identification and analysis of vascular tree structures in retinal vessel network. Proceedings of SPIE, 2011, , .	0.8	12
45	Automated 3-D method for the correction of axial artifacts in spectral-domain optical coherence tomography images. Biomedical Optics Express, 2011, 2, 2403.	1.5	67
46	Robust Multiscale Stereo Matching from Fundus Images with Radiometric Differences. IEEE Transactions on Pattern Analysis and Machine Intelligence, 2011, 33, 2245-2258.	9.7	34
47	Vessel Boundary Delineation on Fundus Images Using Graph-Based Approach. IEEE Transactions on Medical Imaging, 2011, 30, 1184-1191.	5.4	93
48	Association of visual function and ganglion cell layer thickness in patients with diabetes mellitus type 1 and no or minimal diabetic retinopathy. Vision Research, 2011, 51, 224-228.	0.7	110
49	Identification and reconnection of interrupted vessels in retinal vessel segmentation. , 2011, , .		13
50	Segmentation of the Optic Disc in 3-D OCT Scans of the Optic Nerve Head. IEEE Transactions on Medical Imaging, 2010, 29, 159-168.	5.4	144
51	Three-Dimensional Analysis of Retinal Layer Texture: Identification of Fluid-Filled Regions in SD-OCT of the Macula. IEEE Transactions on Medical Imaging, 2010, 29, 1321-1330.	5.4	186
52	Automated Segmentation of Neural Canal Opening and Optic Cup in 3D Spectral Optical Coherence Tomography Volumes of the Optic Nerve Head. , 2010, 51, 5708.		79
53	Automated 3D segmentation of intraretinal layers from optic nerve head optical coherence tomography images. Proceedings of SPIE, 2010, , .	0.8	20
54	Retinal Imaging and Image Analysis. IEEE Reviews in Biomedical Engineering, 2010, 3, 169-208.	13.1	1,021

#	Article	IF	CITATIONS
55	Decreased Retinal Ganglion Cell Layer Thickness in Patients with Type 1 Diabetes. , 2010, 51, 3660.		294
56	Automated Segmentation of 3-D Spectral OCT Retinal Blood Vessels by Neural Canal Opening False Positive Suppression. Lecture Notes in Computer Science, 2010, 13, 33-40.	1.0	18
57	Automated segmentation of the optic disc margin in 3-D optical coherence tomography images using a graph-theoretic approach. Proceedings of SPIE, 2009, , .	0.8	18
58	Registration of 3D spectral OCT volumes using 3D SIFT feature point matching. Proceedings of SPIE, 2009, , .	0.8	29
59	Automated Segmentation of the Cup and Rim from Spectral Domain OCT of the Optic Nerve Head. , 2009, 50, 5778.		82
60	Intraretinal Layer Segmentation of Macular Optical Coherence Tomography Images Using Optimal 3-D Graph Search. IEEE Transactions on Medical Imaging, 2008, 27, 1495-1505.	5.4	300
61	Vessel segmentation in 3D spectral OCT scans of the retina. , 2008, , .		46